

Photoemission Investigation of the Band Structure of Ferromagnetic Ni-Al Alloys*†

W. M. BREEN‡ AND F. WOOTEEN

*Department of Applied Science and Lawrence Radiation Laboratory,
University of California, Livermore, California*

AND

T. HUEN

Lawrence Radiation Laboratory, University of California, Livermore, California

(Received 9 November 1966)

Photoemission measurements probing the electronic band structure of ferromagnetic Ni-Al alloys have been made with ultraviolet light, from 4.5 to 11.4 eV, to determine the optical density of electronic states down to about 6 eV below the Fermi level. Photoemission data were taken at room temperature on two Ni-Al alloys of compositions 92.0 and 95.4 at. % Ni. The results are interpreted in terms of the rigid-band model and scattering phenomena. The optical density of states is assumed to be the same for all the Ni-Al alloys investigated. Results obtained from a pure Ni sample cleaned by argon bombardment and heat treatment are the same as those of Blodgett from a pure Ni sample formed by evaporation onto a substrate.

I. INTRODUCTION

AN understanding of ferromagnetism in the transition metals and their alloys requires knowledge of the electronic density of states of these materials. A number of experimental techniques exist for studying the Fermi surface, but a knowledge of the entire band structure below the Fermi surface is required. Soft x-ray emission and absorption, optical reflectivity, photoelectric emission, and most recently, ion-neutralization spectroscopy, provide information about the density of electronic states away from the Fermi surface. Each method has its own advantages and disadvantages. Results from ferromagnetic alloys of Ni-Al reported in this paper are derived from the photoelectric-emission technique. That is, the energy distribution and quantum yield of emitted photoelectrons were measured and the results interpreted in terms of electronic band structure and scattering mechanisms. The theory behind this method is presented in Sec. II in terms of a simple physical model. Experimental description is given in Sec. III.

Why study Ni-Al alloys? First, no one has used the photoemission technique to study alloys. On the other hand, Ni and Cu have been studied¹⁻⁶ and the results

* Work performed under the auspices of the U. S. Atomic Energy Commission.

† Based on a dissertation submitted by W. M. Breen to the University of California, Davis, in partial fulfillment of the requirements of the Ph.D. degree.

‡ Captain, U.S. Air Force. Present address: U.S. Air Force Weapons Laboratory, Kirtland Air Force Base, Albuquerque, New Mexico.

¹ A. J. Blodgett, Jr., and W. E. Spicer, *Phys. Rev. Letters* **15**, 29 (1965).

² A. J. Blodgett, Jr., and W. E. Spicer, *Phys. Rev.* **146**, 390 (1966).

³ W. E. Spicer, in *Optical Properties and Electronic Structure of Metals and Alloys*, edited by F. Abeles (North-Holland Publishing Company, Amsterdam, 1966), p. 295.

⁴ C. N. Berglund and W. E. Spicer, *Phys. Rev.* **136**, A1030 (1964).

⁵ C. N. Berglund and W. E. Spicer, *Phys. Rev.* **136**, A1044 (1964).

⁶ C. N. Berglund, in *Optical Properties and Electronic Structure of Metals and Alloys*, edited by F. Abeles (North-Holland Publishing Company, Amsterdam, 1966), p. 285.

were quite interesting: The band structure of Cu and Ni as inferred from photoemission measurements could not be related via the rigid-band model, and there appears to be a surprising high-density peak in the density of states of Ni about 4.6 eV below the Fermi level. The question then arises: Is the difference between Ni and Cu a result of differences in the number of *s*- and *p*-like electrons, or does it depend upon whether or not the *d* states are filled, or upon many-body effects lying outside conventional band theory? What will happen when the *d* states of Ni are filled in by alloying? To shed some light on these questions a study of ferromagnetic Ni-Al alloys was undertaken. (Ni-Cu alloys are currently being studied by Spicer and Seib.)⁷ Aluminum has an advantage as an additive in that it has no *d* states of its own to contribute to the valence band of the alloy. Experiments on magnetization in Ni-Al indicate that Al serves primarily only as a source of electrons for filling the Ni *d* states.⁸⁻¹⁰

The nickel-rich side of the Ni-Al alloy system was investigated at two different single phase compositions (92.0 and 95.4 at. % Ni). Experimental data were also taken on pure Ni to check existing data obtained by photoemission with an evaporated Ni sample.^{1,2} Data presented in Sec. IV were taken at room temperature with photons having energies up to 11.4 eV. This allows probing the electronic states down to 6 or 7 eV below the Fermi level. All samples were ferromagnetic, but possessed different Curie temperatures because of their different compositions.

Interpretation of the data in terms of various theoretical models is made in Sec. V. The optical density of electronic states determined from photoemission data is presented and compared with theoretical calculations

⁷ W. E. Spicer and D. Seib (private communication).

⁸ E. C. Stoner, *Phil. Mag.* **15**, 1018 (1933).

⁹ N. F. Mott and H. Jones, *The Theory and Properties of Metals and Alloys* (Clarendon Press, Oxford, England, 1936; reprinted by Dover Publications, Inc., New York, 1958).

¹⁰ J. Crangle and M. J. C. Martin, *Phil. Mag.* **4**, 1006 (1959).

made by others.^{11,12} Alloy data are interpreted in terms of electron-phonon and electron-electron scattering phenomena. Emphasis is placed on interpretation of differences between Ni and Ni-Al alloys rather than on an absolute interpretation of the data.

II. THEORY

Photoemission from metals is a two-step process: photoexcitation, and the escape of the excited electron from the material. The light used in experiments typically ranges in energy from the work function of the material (about 5 eV for most metals) to the vacuum ultraviolet (up to 11.4 eV in this work). Light is mostly absorbed within a few hundred angstroms, exciting electrons into unfilled states above the Fermi level. Electrons with energies greater than the vacuum level, i.e., the Fermi level plus the work function, are then free to escape the emitter if they arrive at the surface within a certain escape cone. Factors determining whether an electron reaches the surface involve interactions such as electron-phonon and electron-electron scattering events. Once the electrons have been emitted into the vacuum their energy distributions may be measured. The energy distribution is related to the density of electronic states and may be used to study details of the energy-band structure if electron excitation, scattering, and escape are reasonably understood.

Photoexcitation, scattering processes, and electron escape are described more thoroughly below. A more complete discussion of some aspects of the problem, especially concerning selection rules for optical transitions is to be found in the papers of Spicer and co-workers.^{1-6,13,14}

A. Photoexcitation

The first step in the photoemission process takes place when the light falls on the emitter. Electrons below the Fermi level are excited to unoccupied states of higher energy. These transitions are often described as direct, indirect, or nondirect. In a direct or vertical transition to a higher unoccupied state caused by interaction with a photon, crystal momentum $\hbar\mathbf{k}$ is conserved. In indirect, or phonon-assisted, transitions the value of \mathbf{k} is conserved by phonons. In addition to the two types of transitions based on the Bloch description, the actual transition in the metal or alloy may be one in which conservation of \mathbf{k} appears not to be an important selection rule. This is called a nondirect transition.

Blodgett and Spicer^{1,2} found that in Ni the conservation of crystal momentum appears not to be important. Crystal momentum is thus either conserved

by unknown processes, is not conserved at all, or a description in terms of \mathbf{k} is not meaningful. Besides Ni, other metals^{3-6,15-17} and semiconductors^{13,18} investigated by the photoemission technique have mostly exhibited nondirect transitions, though evidence for some direct transitions has been seen.

When photoexcitation is accomplished by indirect or nondirect transitions, the probability of exciting an electron is proportional to the product of the initial and final densities of states^{1,2}:

$$P(E) = CN_e(E)N_v(E-h\nu), \quad (1)$$

where $P(E)$ is the probability per unit energy interval of exciting an electron from an initial state at energy $E-h\nu$ to a final state at energy E ; C is a coefficient (assumed to be constant) which includes the square of matrix elements connecting the initial and final states; $N_e(E)$ is the density of unoccupied states above the Fermi level at energy E ; and $N_v(E-h\nu)$ is the density of occupied states below the Fermi level at energy $E-h\nu$. The assumption of constant matrix elements enables photoemission data to be readily interpreted to first order¹⁻⁶ in a self-consistent manner. Second-order discrepancies in the data may then be associated with this assumption among others.

B. Scattering Processes

Once the electrons are excited to higher-energy states they may be subject to scattering processes prior to escape. The two main interactions the photoelectrons may undergo in this energy range are electron-phonon and electron-electron scattering events.

The interactions of photoelectrons with phonons are nearly elastic. They do not change the energy of electrons to an extent observable by photoemission. They do, however, affect the escape probability.¹⁹ Electrons near the surface may have more chance to escape if they undergo many electron-phonon collisions. This can happen because an electron that reaches the surface and does not escape, but is reflected back into the material, can then be redirected towards the surface by additional scattering and may have several more chances to escape. On the other hand, electrons which stay within a small region of the sample for a longer time because of electron-phonon collisions are subject to an increasing probability of undergoing inelastic scattering processes, e.g., electron-electron collisions, and never reaching the surface. Which effect dominates depends upon the relative magnitudes of the mean optical ab-

¹⁵ A. J. Blodgett, Jr., W. E. Spicer, and A. Y-C. Yu, in *Optical Properties and Electronic Structure of Metals and Alloys*, edited by F. Abeles (North-Holland Publishing Company, Amsterdam, 1966), p. 246.

¹⁶ W. E. Spicer, J. Appl. Phys. **37**, 947 (1966).

¹⁷ F. Wooten, T. Huen, and R. N. Stuart, in *Optical Properties and Electronic Structure of Metals and Alloys*, edited by F. Abeles (North-Holland Publishing Company, Amsterdam, 1966), p. 333.

¹⁸ N. B. Kindig and W. E. Spicer, Phys. Rev. **138**, A561 (1965).

¹⁹ R. N. Stuart and F. Wooten, Phys. Rev. **156**, 364 (1967).

¹¹ J. Yamashita, M. Kukuchi, and S. Wakoh, J. Phys. Soc. Japan **18**, 999 (1963).

¹² L. F. Mattheis, Phys. Rev. **134**, A970 (1964).

¹³ W. E. Spicer, Phys. Rev. Letters **11**, 1 (1963).

¹⁴ W. E. Spicer, Phys. Letters **20**, 325 (1966).

sorption depth and the mean free paths for electron-electron and electron-phonon scattering.

Electron-electron interactions take place between photoexcited electrons and electrons still in the ground state. An energy equal to the difference between the state of the photoelectron before and after scattering is exchanged. Since both the photoelectron and ground-state electron must go to unoccupied states after the collision, events are most probable in which much of the excitation energy above the Fermi level is lost by the photoelectron. The effect is even more enhanced in Ni by the high density of unoccupied states just above the Fermi level (Fig. 10). It is most probable, therefore, that the photoelectron will lose enough energy so that either it or the electron it interacts with will end up in one of the high-density unoccupied d states. Thus, a large amount of energy is lost in the scattering process. The energy with which an electron escapes from the material and even the probability of escape are greatly affected by the extent of the electron-electron collisions. Usually, the energy distribution is skewed towards lower energies because of electron scattering.

C. Escape

Escape is determined primarily by two factors: (1) one which limits the escaping electrons to an escape cone whose size depends on the photoelectron's vector momentum; and (2) one which accounts for elastic scattering.

The two factors taken together make up an escape function that rises quickly with energy from zero at the vacuum level to a plateau at approximately 2 eV above the vacuum level.² When this escape function is multiplied by the probability of excitation given in Eq. (1), the result is the energy distribution of the emitted electrons (neglecting for the moment the effect of electron-electron scattering);

$$N(E) = CS(E)N_e(E)N_v(E-h\nu), \quad (2)$$

where $N(E)$ is the energy distribution of emitted photoelectrons, and $S(E)$ is the escape function. A few eV above the vacuum level the energy distribution is, therefore, almost the product of the initial and final density of photoelectron states.

It is possible to determine $S(E)$ or, at least, the product $S(E)N_e(E)$ by an iterative procedure from the experimental data.² If inelastically scattered electrons make only a small contribution to the external photoelectron energy distribution, then Eq. (2) provides a simple basis for determining the density of states.

When electron-electron scattering becomes important, an analytical approximation may be used to estimate the contribution of inelastic scattering to the external energy distribution.^{4,5} Another procedure is to explicitly include both electron-electron and electron-phonon scattering in a Monte Carlo analysis.¹⁷ However,

the emphasis in this paper is on a description of the experiment and interpretation of the data in terms of the rigid-band model.

III. EXPERIMENTAL TECHNIQUES

The techniques used in the measurements of energy distribution and quantum yields were, in the main, similar to the ones developed by Spicer *et al.*^{2,5,20} Only a brief description of the techniques is presented here. However, the problems arising from the use of Ni-Al alloys are described more fully, particularly those problems associated with sample preparation and surface treatment.

A. Photoemission Measurements

Both the quantum yield and the energy-distribution measurements were made using a cylindrical collector-emitter assembly at pressures of about 10^{-9} Torr. The energy distribution was measured using the retardation potential and ac-modulation method.²⁰ Two additional modifications were made. The necessity and the resultant advantages of the modifications are described elsewhere.²¹

Relative light intensities were measured using sodium-salicylate-coated photodiodes and photomultipliers.²² A nitric oxide ionization chamber, obtained from Mel-par Company, was used to measure the absolute light intensity at the Lyman- α wavelength (1216 Å). The spectral reflectance $R(\lambda)$ as measured for pure Ni was assumed for all samples.²³ The errors thus introduced into the calculations of the absolute quantum yields (electrons emitted per photon absorbed) are small in view of the type of information wanted.

B. Sample Preparation

Three 50-g Ni-Al alloy samples were made which had starting compositions of 93, 96, and 100 at. % Ni. These samples were arc-melted in an argon atmosphere, cooled, turned over, and remelted. This process was repeated twice. The alloys then were wrapped in Ta foil and underwent a "homogenizing" anneal at 1350°C for 24 h in vacuum furnace. Since the cool-down time of this furnace was long, from 4 to 5 h, a trace of the Ni₃Al phase was able to precipitate out, forming a two-phase sample. To eliminate the Ni₃Al phase, the alloys were vacuum sealed in R-237 alloy cups, annealed at 1175°C for 1 h, and then quenched in water.

After quenching, the alloys were rolled to a thickness of $\frac{1}{8}$ in. The rolling action improves the homogeneity by breaking up any precipitated phase present. Tests showed less than 1% precipitated Ni₃Al phase. The

²⁰ W. E. Spicer and C. N. Berglund, *Rev. Sci. Instr.* **35**, 1665 (1964).

²¹ T. Huen, *Rev. Sci. Instr.* (to be published).

²² R. Allison, J. Burns, and A. J. Tuzzolino, *J. Opt. Soc. Am.* **54**, 747 (1964).

²³ H. E. Ehrenreich, H. R. Phillip, and D. J. Olechna, *Phys. Rev.* **131**, 2469 (1963).

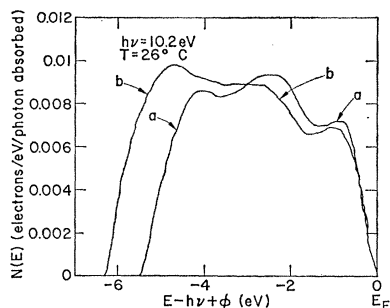


FIG. 1. Energy-distribution curves from pure Ni taken (a) before and (b) after argon-bombardment cleaning operation.

samples were again sealed in R-237 cups, annealed at 1175°C for 1 h to remove mechanical strains, then quenched.

To prepare the alloy samples for use as photoemitters, they were cut to a size of $\frac{1}{8}$ in. \times $\frac{1}{2}$ in. \times $\frac{3}{4}$ in. The emission surface was prepared by electropolishing. The solution used was: 60 ml perchloric acid, 60%, specific gravity 1.54, 600 ml methanol, and 360 ml butylcellosolve. The final compositions, as determined by chemical analysis, are listed below in at. % of Ni.

Starting composition	Final chemical analysis
93	92.0 \pm 0.7
96	95.4 \pm 0.3

The pure Ni sample was prepared to the same size. The surface was lapped with 600-grit papers, followed by hand polishing with 1600-grit paste. It was annealed at 800°C for 30 min to remove strains. The sample was then polished, reannealed, and electropolished to a smooth bright surface. The electropolishing was done with a solution of dilute H₂SO₄ and perchloric acid for 1 min.

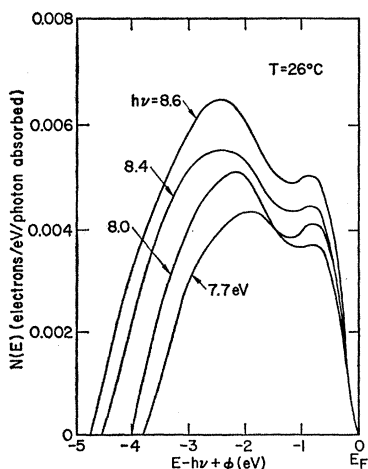


FIG. 2. Energy-distribution curves for electropolished Ni after argon-bombardment cleaning.

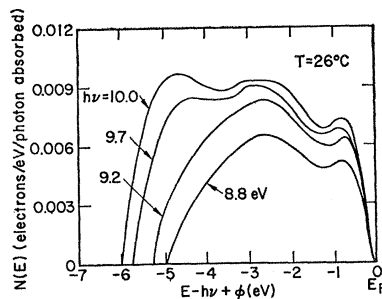


FIG. 3. Energy-distribution curves for electropolished Ni after argon-bombardment cleaning.

C. Surface Treatment

An ion-bombardment technique^{24,25} was used to remove contaminants from the surface of the emitter after it was mounted in the high-vacuum phototube assembly. Argon gas was injected into the chamber by a leak valve until a pressure of about 200 μ was recorded. A glow discharge was initiated with 500-V dc applied between the cylindrical collector and the emitter. An ion current of between 1 to 5 mA was maintained for 5 min. The argon was then pumped out of the chamber by both a "sorption" pump and a Varian vacuon pump. Pressure of about 10⁻⁹ Torr was usually reached.

The argon ions knock contaminants off the emitter surface. At the same time, they also bury themselves in the sample up to a depth of 15 at. layers.²⁶ Hence, the emitter was heated to 400°C by a heater filament placed next to it to drive off the embedded argon. This technique of heating following argon bombardment has been used elsewhere to prepare clean, ordered surfaces for electron-diffraction experiments.²⁷ Besides driving argon from the surface, the heat treatment also anneals the sample and restores the structural order that the bombarding ions had partially destroyed. That the embedded argon was driven off was confirmed

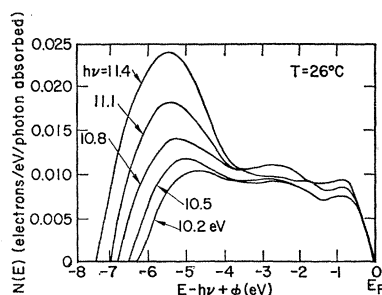


FIG. 4. Energy-distribution curves for electropolished Ni after argon-bombardment cleaning.

²⁴ H. D. Hagstrum and C. D'Amico, *J. Appl. Phys.* **31**, 715 (1960).

²⁵ E. Menzel, in *Reports on Progress in Physics*, edited by A. C. Stickland (The Institute of Physics and the Physical Society, London, 1963), p. 47.

²⁶ J. E. Carmichael and E. A. Trendelenburg, *J. Appl. Phys.* **29**, 1570 (1958).

²⁷ H. E. Farnsworth, R. E. Schlier, T. H. George, and R. M. Burger, *J. Appl. Phys.* **26**, 252 (1955); **29**, 1150 (1958).

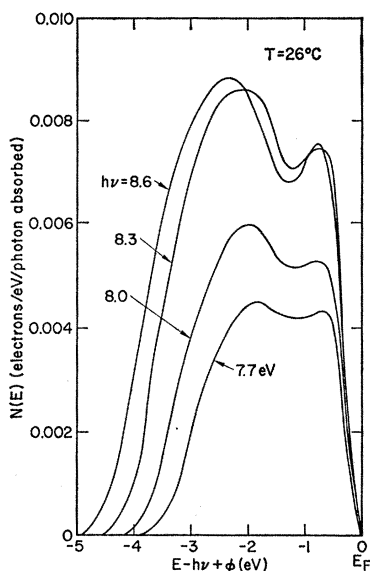


FIG. 5. Energy-distribution curves for 92.0% Ni alloy.

by the different shape of the energy-distribution curve after heat treatment. The ion-bombardment-heat-treatment cycle was repeated several times for each sample until the energy-distribution curves remained constant. A further check of the cleanliness of the surface was possible by a comparison of the results obtained with that obtained by pure Ni thin-film evaporation.

IV. PHOTOEMISSION DATA

Photoemission data from Ni and Ni-Al alloys are shown in Figs. 1-8. The reference level in these energy-distribution curves is taken at the Fermi energy. That is, all measured energy-distribution curves are referred to the initial states by subtracting the photon energy from the sum of external kinetic energy and work function of the emitter. The ordinate is the absolute differential quantum efficiency, i.e., the quantum efficiency per unit energy interval.

It is noticed in all energy distribution data presented here that the low-energy portion of the curves appears to tail off. This is due to a reverse current caused by light reflected from the emitter onto the collector. It is small compared with the forward current and affects only the low-energy portion of the energy-distribution curves.

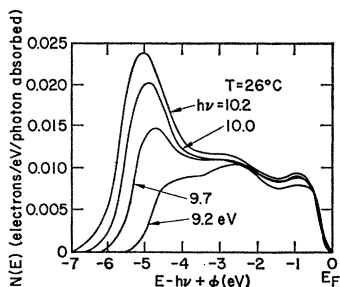


FIG. 6. Energy-distribution curves for 92.0% Ni alloy.

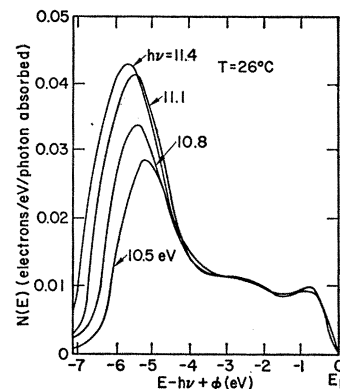


FIG. 7. Energy-distribution curves for 92.0% Ni alloy.

The work function of the pure Ni sample as determined from a Fowler plot^{5,28} was 4.5 ± 0.1 eV. For the two alloy samples the work function was 4.5 ± 0.2 eV.

Photoemission data from pure Ni are shown in Figs. 1-4. The effect of cleaning the surface may be seen in Fig. 1. Curve (a) is before cleaning, and curve (b) is after cleaning. Six cleaning cycles were employed. The work function of the emitter is lower by almost 1 eV after cleaning. An important point is that the main result of a lower work function is simply to allow more structure in the density of states to be revealed. This means that in the present experiments, the results are not appreciably distorted by the surface condition of the sample.

The photoemission data from pure bulk Ni after cleaning are nearly identical with those from evaporated Ni films,^{1,2} so that the combination of argon bombardment and heat treatment is deemed sufficient to produce a clean surface on the alloy samples.

Photoemission data were taken on the pure Ni emitter at two other temperatures, -90 and 150°C . These data are not reproduced here because they varied little from the room-temperature results. They were measured to see if such temperature-dependent phenomena as phonon scattering played a role.

Photoemission data at room temperature for the 92% Ni alloy are presented in Figs. 5-7. The middle- and high-energy peaks are almost the same as the pure

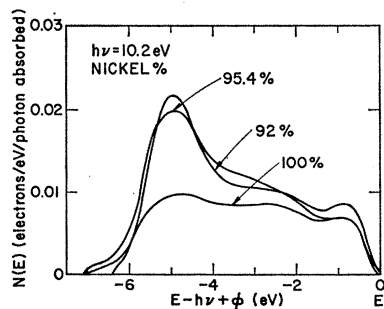


FIG. 8. Energy-distribution curves for photon energy $h\nu = 10.2$ eV.

²⁸ R. H. Fowler, Phys. Rev. **38**, 45 (1931).

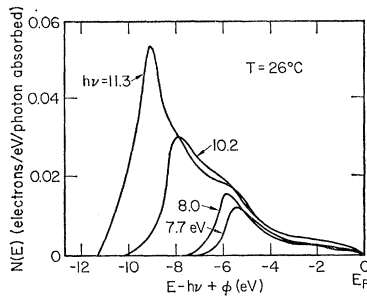


Fig. 9. Energy-distribution curves for 92.0% Ni alloy coated with Cs.

Ni peak heights. The low-energy peak, however, is almost twice as high as that for pure Ni. The sharper structure apparent in Figs. 5–7 is a result of an improvement in the resolution of the electronics system²³ made just before this sample (the last of the series) was studied.

The data from the other two alloy samples are not reproduced here in full, but Fig. 8 shows data taken at the same photon energy (10.2 eV) for all samples. The main features are the same for all samples, except that the low-energy peak is more pronounced the greater the Al concentration.

To permit probing deeper into the valence band, a surface layer of cesium was evaporated onto the 92% Ni alloy and a set of four energy-distribution curves was taken (Fig. 9). The energy-distribution curves appear distorted in much the same way as found by Blodgett²⁹ in studies of Ni with a surface layer of Cs, except for the important point that here the positions of the peaks are not changed by the addition of Cs.

V. DISCUSSION

Photoemission data presented in Sec. IV are here discussed in terms of various theoretical models. Comparison of the experimental density of states is made with some theoretical calculations of the band structure. Interpretation of the results of alloying small amounts of Al with Ni is made in terms of the rigid-band model and scattering.

A. Density of States

Photoemission data presented in Sec. IV for pure Ni can be used to derive an optical density of states, following the procedure outlined in Sec. II. (The optical density of states is the true density of states as modified by the assumption of constant matrix elements and any relaxation effects which may accompany the optical excitation.) Blodgett and Spicer^{1,2} did this by using data on a vacuum-evaporated Ni sample, and derived the optical density of states shown in Fig. 10. The

constant density of states above 0.5 eV in the plot actually continues out to about 11 eV. It is omitted from the figure for convenience.

In Fig. 10, the low-energy peak is the dominant feature of the optical density of states. Calculations of the density of states for Ni do not predict any such low-energy structure.^{11,12,30} All predict a narrow band of less than 2 eV having two peaks with a strong minimum between them. The photoemission determination of the optical density of states is, therefore, in distinct disagreement with these calculations. Immediately the question is then raised as to whether the low-energy peak observed in photoemission does not really arise from electron-electron scattering. This point has been discussed by Blodgett and Spicer¹⁻³ as well as by Phillips.³¹ Their conclusions are that the peak is real and is not primarily due to electron-electron scattering. However, it might be due to many-body effects rather than to a peak in the band-structure density of states.

The present experiments do not shed any new light on the importance of the contribution of electron-electron scattering to the low-energy peak, nor is any new evidence available concerning whether the low-energy peak really represents band-structure or many-body effects. However, data from the 92% Ni alloy with a surface layer of cesium (Fig. 9) do contribute new evidence as to the reality of a low-energy peak in the optical density of states. The shoulder in $N(E)$ appearing near -5 eV for photon energies of 10.2 and 11.3 eV is clearly associated with the low-energy peak in the optical density of states. The structure in $N(E)$ near -9 eV for $h\nu=11.3$ eV is interpreted as arising from electron-electron scattering. Scattering also contributes to the height of the shoulder near -5 eV and must contribute to the low-energy peak observed in pure Ni. The important point, though, is that the data presented in Fig. 9 demonstrate that at least part of the structure near -5 eV arises from real structure in the optical density of states, where now the term "optical density of states" should be understood to include possible many-body effects.

It should be noted that the evidence from photoemission for a peak in the density of states 5 eV below the Fermi level is in direct disagreement with x-ray

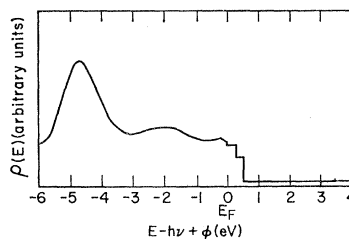


Fig. 10. Optical density of states for Ni and Ni-Al alloys (Refs. 1 and 2). Curve may be considered constant out to 11 eV above E_F .

²⁹ A. J. Blodgett, Jr., Ph.D. dissertation, Stanford University, Stanford, California, 1965 (unpublished).

³⁰ N. F. Mott, *Advan. Phys.* **13**, 325 (1964).

³¹ J. C. Phillips, *Phys. Rev.* **140**, A1254 (1965).

emission data³² and ion-neutralization experiments³³ as well as with theoretical calculations. These differences have yet to be resolved; only tentative explanations have been suggested.^{3,34,35}

B. Ni-Al Alloys

The energy-distribution curves for the Ni-Al alloys are essentially the same as those for pure Ni. The only significant difference is in the relative heights of the low-energy peak, the peak height increasing with aluminum concentration. Since the rigid-band model provides an adequate basis for explaining the magnetic behavior of Ni-Al alloys,^{8-10,36} it is important to see if the photoemission data can be explained in like manner.

Assuming that the density of states does not change with aluminum concentration for the dilute Ni-Al alloys investigated here, the peak locations in the energy distribution curves should change very little. Only small changes associated with filling in the d states should take place. The extent of these changes is too small to be resolvable in these experiments. The main effect is simply that the magnitudes of the low-energy peaks differ.

It is believed that the greater height of the low-energy peak for the Ni-Al alloys is a result of additional scattering, not a significant change in the density of states. The explanation is quite simple. First, the addition of aluminum results in some of the empty d states become filled. This, in turn, increases the relative probability that an electron will be scattered to a state above the vacuum level. Second, there is a greater contribution from phonon scattering or other elastic-scattering events. That is, if an electron is scattered inelastically to some state above the vacuum level, it has a greater escape probability from the alloys than from pure Ni because of increased elastic scattering

in the alloys. This arises (as discussed in Sec. II) because an electron which reaches the surface but does not escape may be redirected towards the surface by elastic scattering and have several more changes to escape.¹⁹ The increase in elastic scattering with aluminum concentration is indicated by the change in electrical resistivity. At room temperature the resistivity of pure Ni is about $8 \times 10^{-6} \Omega \text{ cm}$, while that of 92% Ni alloy is about $30 \times 10^{-6} \Omega \text{ cm}$.³⁷

There are other factors which may contribute to the increased height of the low-energy peak in the Ni-Al alloys. It may be that the transition probability for excitation from the low-energy peak in the density of states (or for many-body excitations) is greater in the alloy even though the density of states itself does not change appreciably. Another possibility is suggested by the x-ray absorption studies on Ni-Al alloys by Das and Azaroff.³⁸ Their work suggests that the rigid-band model is followed at least qualitatively for Al concentrations up to 5.5 at.%. At concentrations of 8.35 at.%, however, there is evidence of an increase in p -type symmetry for states just above the Fermi energy. They suggest that there may be a tendency to form hybridized orbitals or, perhaps, overlapping of Al p orbitals leading to localized deviations from the rigid-band model. A change in bond character of the unfilled states just above the Fermi energy would lead to some change in the scattering cross section. The point is, then, that there are various possibilities for transition matrix elements to differ among the different alloys and pure Ni, but the simplest explanation is just that the rigid-band model is essentially valid and that the increase in peak height is due primarily to a change in scattering.

ACKNOWLEDGMENTS

We gratefully acknowledge helpful discussions of the experiments with W. E. Spicer. We wish to thank R. J. Borg and P. R. Landon for valuable experimental suggestions, D. W. Brown for his help in fabricating the alloys, and R. E. Brandt for chemical analysis. J. A. Pastrone and P. H. Jacob were of considerable help in designing and assembling portions of the experimental apparatus.

³² R. O. Williams, *Trans. AIME* **215**, 1026 (1959).

³³ B. N. Das and L. V. Azaroff, *Acta Met.* **13**, 827 (1965).

³² Y. Cauchois and C. Bonnelle, in *Optical Properties and Electronic Structure of Metals and Alloys*, edited by F. Abeles (North-Holland Publishing Company, Amsterdam, 1966), p. 83.

³³ H. D. Hagstrum, *Phys. Rev.* **150**, 495 (1966).

³⁴ N. F. Mott, comments at end of paper by W. E. Spicer (Ref. 3).

³⁵ J. R. Cuthill, A. J. McAlister, and M. L. Williams, *Phys. Rev. Letters* **16**, 993 (1966).

³⁶ G. S. Krinchuk and E. S. Banin, *Zh. Eksperim. i Teor. Fiz.* **49**, 470 (1965) [English transl.: *Soviet Phys.—JETP* **22**, 331 (1966)].